EDITORS

PROF. DR. IRINA-ANA DROBOT
PROF. DR. HABİBE ÖZMEN

26TH INTERNATIONAL ISTANBUL SCIENTIFIC RESEARCH CONGRESS ON LIFE, ENGINEERING, ARCHITECTURE, AND MATHEMATICAL SCIENCES PROCEEDINGS BOOK

AUGUST 18-20, 2026
İSTANBUL, TÜRKİYE



PARTICIPANT COUNTRIES (24 COUNTRIES)

Albania • Algeria • Azerbaijan • Bangladesh • China • Ethiopia • Hungary • India • Iran • Iraq • Kosovo • Libya • Malaysia • Morocco • Namibia • Nigeria • Pakistan • Philippines • Poland • Portugal • Saudi Arabia • Spain • Sudan • United States of America

E-ISBN: 978-9952-610-87-1
DOI: **https://doi.org/10.30546/19023.978-9952-610-87-1.2026.100.1144.**

OTURUM (1) | GÜN (2) | SALON (4) – SESSION (1) | DAY 2) | HALL (4)

Kabatas Salonu | Kabatas Hall

MEETING ID: 813 8841 5830
PASSWORD: 505041

	19.08.2026	Time: 10^{00}-13^{30} (Turkey Local time GMT+3)	MODERATOR & HEAD OF SESSION: *O. Fevzi YAMAN* COORDINATOR & CO-COORDINATOR: *Baha Ahmet YILMAZ*
	Authors	**Affiliation**	**Topic title**
10^{00}-10^{15}	O. Fevzi YAMAN	*Afyon Kocatepe University, Türkiye*	ERROR, UNCERTAINTY, AND MODEL VALIDITY IN THE EXPERIMENTAL–NUMERICAL VALIDATION OF HONEYCOMB SANDWICH STRUCTURES
10^{15}-10^{30}	O. Fevzi YAMAN	*Afyon Kocatepe University, Türkiye*	EFFECT OF CARBON NANOTUBE PLACEMENT ON THE MECHANICAL PERFORMANCE OF SANDWICH COMPOSITES: A COMPARISON OF FACE-SHEET, CORE, AND INTERFACE STRATEGIES
10^{30}-10^{45}	Murat KAYA	*Independent Researcher, Türkiye*	INVESTIGATION OF THE EFFICIENCY OF A SOLAR-POWERED THERMOELECTRIC GENERATOR
10^{45}-11^{00}	Erdem DELİAĞAOĞLU Tülin ŞAHİN Gurer KUTLUG Malik ARSLAN	*Bericap Kapak San. A.Ş, Türkiye* *Kocaeli University, Türkiye* *Bericap Kapak San. A.Ş, Türkiye* *Bericap Kapak San. A.Ş, Türkiye*	DEVELOPMENT OF POLYETHYLENE-BASED BIODEGRADABLE CLOSURE MATERIAL
11^{00}-11^{15}	Erdem DELİAĞAOĞLU Tülin ŞAHİN Gurer KUTLUG Malik ARSLAN	*Bericap Kapak San. A.Ş, Türkiye* *Kocaeli University, Türkiye* *Bericap Kapak San. A.Ş, Türkiye* *Bericap Kapak San. A.Ş, Türkiye*	DEVELOPMENT OF A POLYPROPYLENE BASED BIODEGRADABLE CLOSURE MATERIAL
11^{15}-11^{30}	Ömer GİLAN Fatih ŞİMŞEK	*Ulaşım İç ve Dış Tic. A.Ş, Türkiye*	MATLAB-BASED HEAT TRANSFER MODELING FOR AIR COMPRESSOR STEEL LINES IN ELECTRIC BUS APPLICATIONS
11^{30}-11^{45}	İsmail GENÇ Yunus KIZILARSLAN	*Ulaşım İç ve Dış Ticaret A.Ş., Türkiye*	POST-PRODUCTION TEST SYSTEMS IN AUTOMOTIVE WIRING HARNESSES: ELECTRICAL, MECHANICAL AND FUNCTIONAL VERIFICATION APPLICATIONS
11^{45}-12^{00}	Muharrem TAŞDEMİR Fatih ŞENASLAN	*Gümüşhane University, Türkiye*	EFFECT OF CURRENT DENSITY ON MICROHARDNESS AND SURFACE ROUGHNESS OF COATING IN ANODIZATION PROCESS OF AZ31 MAGNESIUM ALLOY
12^{00}-12^{15}	Ünal AKDAĞ Soefou Omar HASSANİ	*Aksaray University, Türkiye*	NUMERICAL STUDY ON THE IMPACT OF PULSED AIR JETS ON THERMAL MANAGEMENT OF LITHIUM-ION BATTERY PACKS
12^{15}-12^{30}	Sertaç COŞMAN Üsame DEMİR Samet ÇELEBİ	*Burdur Mehmet Akif Ersoy University, Türkiye* *Bilecik Şeyh Edebali University, Türkiye* *Sakarya University of Applied Sciences, Türkiye*	COMPARATIVE NOISE AND VIBRATION ASSESSMENT OF DIESEL FUELS BLENDED WITH A PALLADIUM(II) THIOUREA COMPLEX UNDER DIFFERENT EGR RATES
12^{30}-12^{45}	Semih ÇELİK Aziz SEZGİN	*Istanbul University-Cerrahpaşa, Türkiye*	GENETIC ALGORITHM-BASED PID PARAMETER OPTIMIZATION FOR A TWO-DEGREE-OF-FREEDOM ROBOTIC ARM
12^{45}-13^{00}	Ferit Sezer YAVUZ Selma AKÇAY	*Cankiri Karatekin University, Türkiye*	ADVANCEMENTS IN HEAT TRANSFER ENHANCEMENT IN SOLAR AIR DUCTS

13^{00}-13^{15}	**Ismail BAYAR** **Huseyin KOSE**	***Batman University, Türkiye***	**EFFECT OF Z-PIN REINFORCEMENT ON INFILL-GEOMETRY-DEPENDENT FLEXURAL BEHAVIOR IN PLA PARTS**
13^{15}-13^{30}	**Yusuf Mert KARAGÖZ** **Duygu İPCİ**	***Gazi University, Türkiye***	**SINGULAR VALUE DECOMPOSITION-BASED GEOMETRIC STABILITY AND MIDDLE AXLE OPTIMIZATION IN 6X6 HEAVY VEHICLES**

26TH INTERNATIONAL ISTANBUL SCIENTIFIC RESEARCH CONGRESS ON LIFE, ENGINEERING, ARCHITECTURE AND MATHEMATICAL SCIENCES
AUGUST 18-20, 2026
İSTANBUL TÜRKİYE

DOI: https://doi.org/10.30546/19023.978-9952-610-87-1.2026.100.1144.
ISBN: 978-9952-610-87-1

SINGULAR VALUE DECOMPOSITION-BASED GEOMETRIC STABILITY AND MIDDLE AXLE OPTIMIZATION IN 6X6 HEAVY VEHICLES

Yusuf Mert KARAGÖZ

Gazi University, Graduate School of Natural and Applied Sciences, Department of Automotive Engineering, 06500 Teknikokullar, Ankara

ORCID ID: https://orcid.org/0000-0002-1187-514X

Doç. Dr. Duygu İPCİ

Gazi University, Faculty of Technology, Department of Automotive Engineering, 06500 Teknikokullar, Ankara

ORCID ID: https://orcid.org/0000-0002-8862-7662

ABSTRACT

Heavy-duty vehicle platforms featuring tandem axles and tactical wheels are subjected to asymmetric loading and significant spatial uncertainties regarding their center of mass throughout their operational lifespan. Determining the middle axle position solely based on a reference center of mass during chassis design compromises the vehicle's rollover and pitch stability under real-world conditions. Design-oriented simulations and iterative numerical methods found in the literature entail high computational costs during the preliminary design phase. In this study, an analytical optimization model based on Singular Value Decomposition (SVD) was developed to directly determine the geometric stability and optimal middle axle placement of hyperstatic vehicle chassis without requiring iterations. A hyperstatic 6x6 heavy-duty vehicle chassis was selected to validate the theoretical approach of the methodology. For the mathematical modeling, the vehicle body was treated as a rigid structure, excluding elastic deformations resulting from torsion or bending within the chassis. A 6-Degree-of-Freedom (6-DOF) Geometric Jacobian matrix was constructed using the coordinates of the vehicle's wheels relative to its center of mass. The system's directional load-bearing capacities were derived by decomposing the geometric matrix into its orthogonal subspaces via the SVD algorithm. The condition number was utilized to optimize the middle axle position amidst uncertainties regarding the vehicle's center of mass. The findings quantify the stability loss inherent in industrial tandem axle architectures and demonstrate that the developed methodology can serve as a rapid, reliable mathematical filter grounded in rigid-body kinematics for vehicle preliminary design processes.

Keywords: Singular value decomposition, geometric stability, hyperstatic chassis, middle axle optimization, condition number.

INTRODUCTION

Heavy-duty wheeled platforms are generally designed in multi-axle (6x6 or 8x8) configurations in the industry due to their high load capacities and mobility in challenging terrain conditions. However, these

DOI: https://doi.org/10.30546/19023.978-9952-610-87-1.2026.100.1144.
ISBN: 978-9952-610-87-1

vehicles are shaped around two basic chassis architectures depending on their intended use and operational priorities. As illustrated in Figure 1 (a), a highly prevalent architecture is the rear-tandem layout, where the rear axles are grouped together. This topology is widely preferred not only in traditional commercial heavy vehicles (e.g., Mercedes-Benz Arocs or MAN TGS) for load-carrying efficiency. But also, in heavy-duty tactical and logistical vehicles (e.g., Renault Sherpa 6x6 variants) or specialized expedition trucks to support heavy rear-mounted shelters or equipment. In contrast, as given in Figure 1 (b) tactical wheeled armored vehicles (TTZA) (e.g., platforms such as FNSS PARS 6x6, Otokar ARMA 6x6, or Oshkosh FMTV) prefer independent suspension architectures where the axles are more separated and evenly distributed to the chassis, in line with the needs of overcoming challenging terrain obstacles and tolerating regional wheel losses in ballistic/mine explosions. Figure 1 shows these two different 6x6 chassis topologies that are commonly used in the market.



(a) Renault Sherpa (b) FNSS PARS

Figure 1. Different chassis configurations in 6x6 vehicles: (a) Commercial heavy vehicle with tandem axle architecture, (b) Tactical wheeled platform with independent axle architecture

Although their architectures differ, the biggest common challenge both vehicle types face in the field is the asymmetric loads, body type changes, heavy weapon/armor integrations, and sloping terrain conditions they are subjected to throughout their operational lives (Liu et al., 2025; Meena & Das, 2025). This variability in operational scenarios leads to a continuous deviation of the vehicle's center of mass (CoG) from its nominal position in three-dimensional space (Liu et al., 2025; Wittmer, Sawodny, & Henning, 2023). Designing the chassis based solely on a fixed ideal center of mass jeopardizes the vehicle's rollover and pitching stability in real-world conditions where the center of mass shifts, narrowing the reliability limits of the design (Wittmer et al., 2023).

In the automotive industry, Multibody Dynamics (MBD) based simulation software is widely used today to determine vehicle dynamics and stability limits (Duraikannu & Dumpala, 2026; Mantaras, Luque, & Alonso, 2022). However, these numerical methods require high computational costs because they rely on time-dependent integration of differential equations, and present the designer with an iterative (trial-and-error) solution process (Cheng et al., 2026). Moreover, establishing high-fidelity vehicle models (such as those used in vehicle-structure interaction or detailed multi-body dynamics) requires pre-defining explicit 3D

DOI: https://doi.org/10.30546/19023.978-9952-610-87-1.2026.100.1144.
ISBN: 978-9952-610-87-1

mechanical properties—including vertical and lateral suspension spring stiffnesses, damper coefficients, axle masses, and chassis moments of inertia (Oliva, Goicolea, Antolín, & Astiz, 2013). In the conceptual design phase, however, these parameters are not yet finalized, preventing designers from receiving quick and reliable mathematical feedback early on when making fundamental topological decisions (Zhou, Kim, & Je Choi, 2020). To avoid these computational costs and parameter dependencies, this study offers a direct analytical alternative using Singular Value Decomposition (SVD) to optimize axle placement and stability in 6x6 heavy vehicles. While previous studies have successfully used Geometric Jacobian matrices to analyze vehicle kinestatics for instance, by evaluating standard 4-wheel suspension mechanisms using screw theory—these approaches heavily depend on detailed suspension parameters that are often unknown during the pre-design phase(Zhou et al., 2020).

The literature of active control systems and independently driven wheel algorithms are frequently employed to enhance the directional stability of multi-axle heavy vehicles. such as external yaw moment control (Hu et al., 2021), sliding mode torque distribution strategies (Xu, Chen, Gao, Jiang, & Feng, 2023) or stability region estimations via sum-of-squares programming (Fang et al., 2025). These dynamic approaches aim to improve outcomes through instantaneous electronic interventions rather than addressing the geometric vulnerabilities inherent to the system. They rely on complex suspension

and inertial parameters that are undefined during the conceptual design phase. In this study addresses the topological stability of a 6x6 chassis through rigid-body kinematics, eliminating the need for any active controllers or algorithmic iterations.

Further extending the matrix based perspective, we consider the hyperstatic 6x6 chassis as a fully independent rigid body(Zhou et al., 2020). The 6-DOF Geometric Jacobian matrix in wheel coordinates defines system stability. The SVD algorithm then provides the natural equilibrium axes of the vehicle without the use of numerical iterations or complex suspension models.

In the geometric literature, a system's sensitivity to distortion and deviation from an ideal reference state is evaluated using the condition number of its Jacobian matrix. The 6-DOF Geometric Jacobian matrix in wheel coordinates defines system stability. The SVD algorithm then provides the natural equilibrium axes of the vehicle without the use of numerical iterations or complex suspension models. The sensitivity of the 6x6 layouts to 3D CM shifts is assessed with condition number (Knupp, 2001). The optimal stable position of the middle axle is found by the condition number optimization strategy.

2. MATHEMATICAL MODEL AND METHODS

The position vectors of the 6x6 vehicle chassis architecture of wheel and the force components acting on the chassis were structured according to ISO 8855 vehicle dynamics coordinate standards to provide a complete integration with the automotive literature in the analysis processes. The wheel indices of the vehicle are shown in Figure 2. In the geometry of the reference vehicle, the front axle is located at a longitudinal coordinate of +2.8 m, the rear axle group is located at coordinates of -1.2 m and -2.6 m; the vehicle's track width is 2.5 m.

DOI: https://doi.org/10.30546/19023.978-9952-610-87-1.2026.100.1144.
ISBN: 978-9952-610-87-1

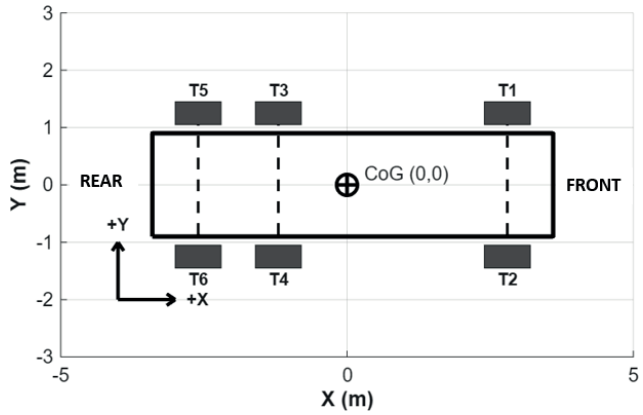


Figure 2. Reference geometric model and wheel indices of a 6x6 heavy-duty vehicle chassis.

The vehicle body is assumed to be a rigid structure; therefore, elastic deformations resulting from torsion or bending in the chassis are excluded from the mathematical model. The static equilibrium of the vehicle is defined by the linear relationship between the wheel reaction forces and the external forces;

$$\mathbf{AF=B}\ . \tag{1}$$

In this equation, **A** represents the geometric Jacobian matrix of the vehicle, **F** denotes the force components acting on the wheels, and **B** represents the external forces. When all wheels are taken into consideration, the general matrix representation of the system can be expressed as:

$$\begin{bmatrix}\mathbf{A}_1 & \mathbf{A}_2 & \cdots & \mathbf{A}_6\end{bmatrix}\begin{bmatrix}\mathbf{F}_1\\ \mathbf{F}_2\\ \vdots\\ \mathbf{F}_6\end{bmatrix}=\begin{bmatrix}\sum F_x\\ \sum F_y\\ \sum F_z\\ \sum M_x\\ \sum M_y\\ \sum M_z\end{bmatrix}. \tag{2}$$

The 6×18 matrix formulated in Equation (2) demonstrates how the 18 force components, summing the reactions in the x, y, and z directions from the all six wheels, affect the 6 fundamental equilibrium states (three translational and three rotational degrees of freedom) at the vehicle's center of mass. The subscripts in the matrix indicate the wheel number. For each wheel, the sub-matrix is defined as follows:

DOI: https://doi.org/10.30546/19023.978-9952-610-87-1.2026.100.1144.
ISBN: 978-9952-610-87-1

$$\mathbf{A}_i = \begin{bmatrix} 1 & 0 & 0 \\ 0 & 1 & 0 \\ 0 & 0 & 1 \\ 0 & -z_i & y_i \\ z_i & 0 & -x_i \\ -y_i & x_i & 0 \end{bmatrix}. \tag{3}$$

2.1. Singular Value Decomposition and Condition Number of Geometric Matrix

By decomposing the chassis's Geometric Jacobian matrix (A) into mutually independent orthogonal subspaces, SVD reveals the system's natural equilibrium axes and the geometric resistance capacity along those axes. The singular value decomposition of the geometric Jacobian matrix A is expressed as follows:

$$[\mathbf{A}]_{6\times 18} = \begin{bmatrix} | & & | \\ u_1 & \cdots & u_6 \\ | & & | \end{bmatrix}_{6\times 6} \begin{bmatrix} \sigma_1 & 0 & \cdots & 0 & \cdots & 0 \\ 0 & \sigma_2 & \cdots & 0 & \cdots & 0 \\ \vdots & \vdots & \ddots & \vdots & \ddots & \vdots \\ 0 & 0 & \cdots & \sigma_6 & \cdots & 0 \end{bmatrix}_{6\times 18} \begin{bmatrix} - & v_1^T & - \\ & \vdots & \\ - & v_{18}^T & - \end{bmatrix}_{18\times 18} \tag{4}$$

The condition number of the geometric matrix is calculated as

$$\kappa = \frac{\sigma_{\max}}{\sigma_{\min}} \tag{5}$$

DOI: https://doi.org/10.30546/19023.978-9952-610-87-1.2026.100.1144.
ISBN: 978-9952-610-87-1

In control allocation, the ideal objective is achieving isotropy ($\kappa = 1$), where forces are transmitted equally in all directions. However, the inherently high aspect ratio of the vehicles results in a high capacity along the longitudinal axis and a much lower capacity along the lateral and roll axes. To overcome the inherent limitations of isotropy-based methods and to account for operational payload uncertainties, a robust min-max optimization strategy is adopted. Although achieving pure isotropy is geometrically impossible for a heavy vehicle due to its high aspect ratio, the algorithm seeks the theoretical minimum of the worst-case condition number within the physical constraints of the chassis.

Mode alignment and matching with physical degrees of freedom

Since SVD algorithm sorts singular values in descending order of magnitude, the direct correspondence between the resulting mathematical modes and the vehicle's physical degrees of freedom (6-DOF) is lost. The column vectors of the left singular matrix $\mathbf{U}$ are used to resolve this structural ambiguity and to provide a physical foundation for the modes. Then the row components of each vector (u_j) define the ratio of the projection of that equilibrium mode onto a certain physical axis

(force or moment). To determine the physical identity of the modes, the maximum projection criterion is used in the following way:

$$m^* = \arg\max\left(\left|u_{m,j}\right|\right), \qquad m \in \{1,\ldots,6\} \tag{6}$$

DOI: https://doi.org/10.30546/19023.978-9952-610-87-1.2026.100.1144.
ISBN: 978-9952-610-87-1

The j-th mode is matched to the m-th physical axis with which it has the highest amplitude. After the mode alignment procedure is completed, these physical correspondences are assigned to thecorresponding singular values (σ_i). Thus, apart from the standard SVD-based sorting, each σ_i value is a measure of the directional load-carrying capacity and mechanical advantage of the chassis structure along that specific task space axis.

3. RESULTS AND DISSCUSSIONS

Figure 3 shows the 6-DOF geometric rigidity indices (SVD Sigma values) for the asymmetric 6x6 chassis configuration with uncertainties of the center of gravity (CoG). This normalization process makes the structural characteristics of the chassis independent of physical scale and thus all degrees of freedom can be compared on a common mathematical plane. The analysis of the graph shows that the rigidity features of the chassis are divided into two major groups:

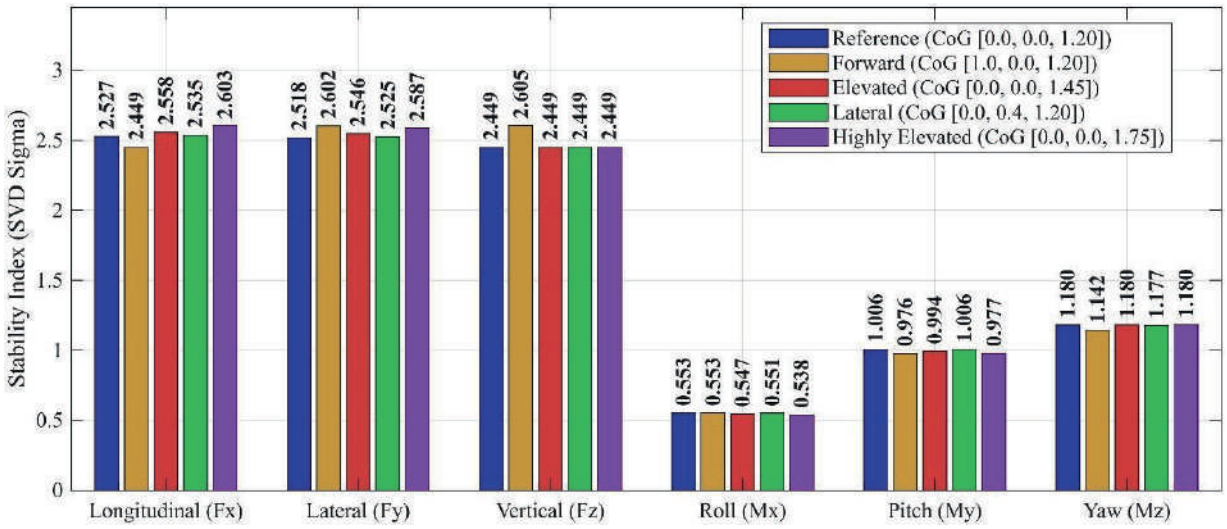


Figure 3. Comparison of the 6-DOF geometric rigidity indices of the 6x6 chassis across with 2.5 m track different center of gravity (CoG) scenarios.

High Stability Zone (Translational Modes): The axes of forces of the longitudinal, lateral and vertical coincide at a level about 2.5, which is the strongest region of the system. The chassis exhibits high geometric stability against translational movements across all four CoG scenarios.

Low Stability Zone (Rotational Modes): The roll, pitch, and yaw moment axes possess considerably lower statbility indices compared to the translational modes. This confirms that the chassis exhibits a geometrically weaker and more flexible character against rotational moments than against translational forces.

DOI: https://doi.org/10.30546/19023.978-9952-610-87-1.2026.100.1144.
ISBN: 978-9952-610-87-1

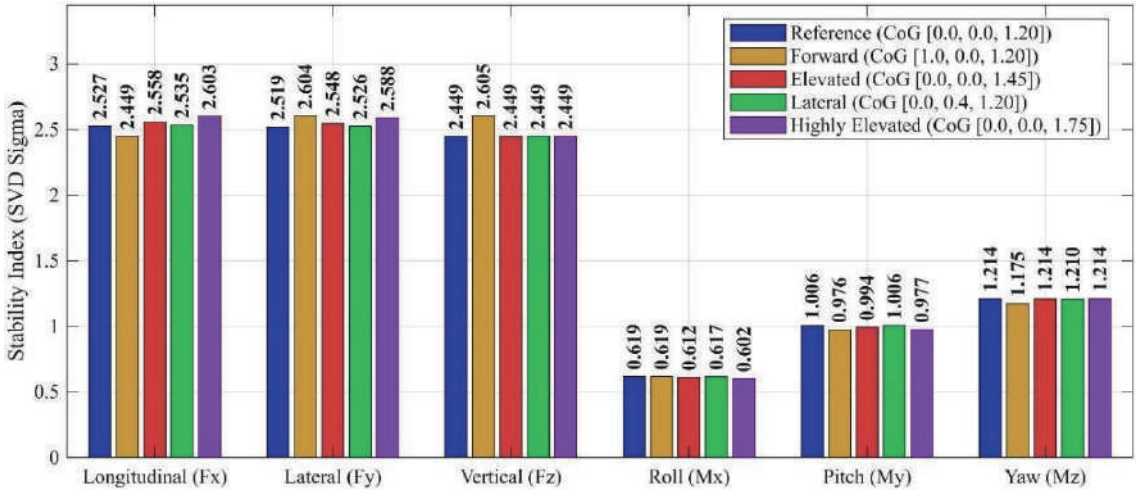


Figure 4. Comparison of the 6-DOF geometric rigidity indices of the 6x6 chassis across with 2.8 m track different center of gravity (CoG) scenarios.

In the scenarios presented in Figure 3 (with a track width of 2.5 m) and Figure 4 (with a track width of 2.8 m), the roll axis remains the parameter with the lowest rigidity index. For the configuration with a track width of 2.5 m, the roll axis geometric rigidity index is approximately 0.55 and grows proportionally with an increase in track width up to 2.8 m. In all configuration, the roll rigidity index does not change even if the center of gravity (CoG) is highly elevated. The vehicle's stabilizing capacity against roll is bounded by its lateral track width. The low rigidity values observed in the SVD analysis are a direct mathematical consequence of this geometric limitation and are independent of the CoG elevation.

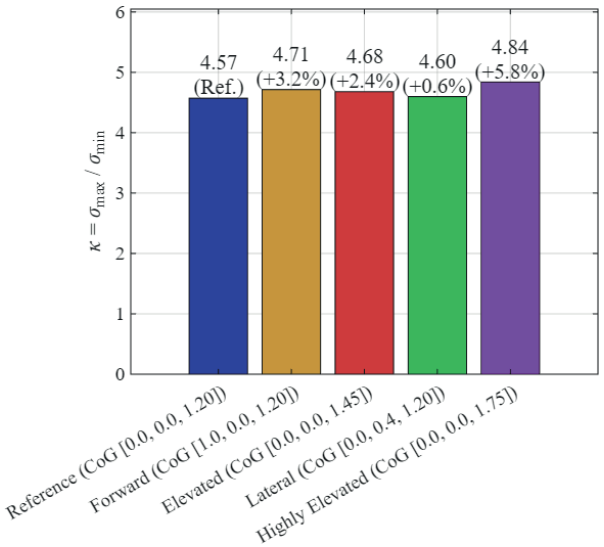


Figure 5. Condition numbers of center of gravity variations

DOI: https://doi.org/10.30546/19023.978-9952-610-87-1.2026.100.1144.
ISBN: 978-9952-610-87-1

Figure 5 presents the condition numbers representing the topological stability and the singularity tendency of the 6x6 chassis under various center of gravity shifts. An increase in this metric indicates a widening gap between the system's strong and weak axes, leading to a degraded load distribution balance.

Compared to the reference state ($\kappa = 4.57$), the highly elevated scenario ($Z = 1.75$ m) caused the most severe degradation, increasing the condition number by 5.8 ($\kappa = 4.84$). This was followed by the longitudinal forward shift of 1.0 m (+3.2%, $\kappa = 4.71$) and the elevated CoG scenario (+2.4%, $\kappa = 4.68$). The lateral shift of 0.4 m exhibited the most limited impact, with a 0.6% increase ($\kappa = 4.60$).

When evaluated against geometric boundaries, the chassis demonstrates higher sensitivity to pitch-direction asymmetries than lateral ones. A longitudinal shift equivalent to 18.5% of the total wheelbase altered the condition number by 3.2%, whereas a lateral shift covering 16% of the track width caused a negligible 0.6% variance. Also, elevating the CoG to 1.75 m deteriorates the stability more than any horizontal translation. This mathematically confirms via the SVD algorithm that vertical CoG placement and the associated dynamic lift-off risks remains the most critical design parameter.

While the adverse effects of a high CoG or asymmetric loading are fundamental facts in vehicle dynamics, the core contribution of the methodology is deriving these dynamic tendencies from the static geometric matrix of wheel coordinates. By solving this topological matrix through Singular Value Decomposition, well-known physical behaviors are translated into a measurable mathematical framework specific to the asymmetric 6x6 chassis. Consequently, this numerical approach not only qualitatively predicts potential risks but quantitatively ranks the disruptive effects of various CoG scenarios, allowing for a precise comparative analysis of the vehicle's weakest modes.

Heavy commercial vehicles and tactical wheeled platforms are subjected to asymmetric loading, chassis type changes, sloping terrain conditions, and varying mission weights throughout their service lives. These operational uncertainties cause the vehicle's center of gravity to deviate from its nominal position. Optimizing the chassis design based on a fixed ideal center of mass will not produce reliable results in real-world conditions. In this context, an optimization strategy was adopted to determine the longitudinal position of the reference chassis' center axle, and the SVD algorithm was run in a 3D design space containing 27 different scenarios where the center of mass could move back and forth, left and right, and up and down. To more comprehensively test the system's stability against uncertainties, analyses were performed for two different operational envelopes: narrow (Figure 6a) and extended (Figure 6b) center of mass boundaries.

The blue dotted line in Fig. 6 (a) and (b) is the nominal CoG ([0,0; 0,0; 1,20]) and the red solid curve shows the worst-case scenario. The shaded pink region is the operational uncertainty band. The optimization objective is to push the peak of this worst-case curve to a global minimum shows maximum instability.

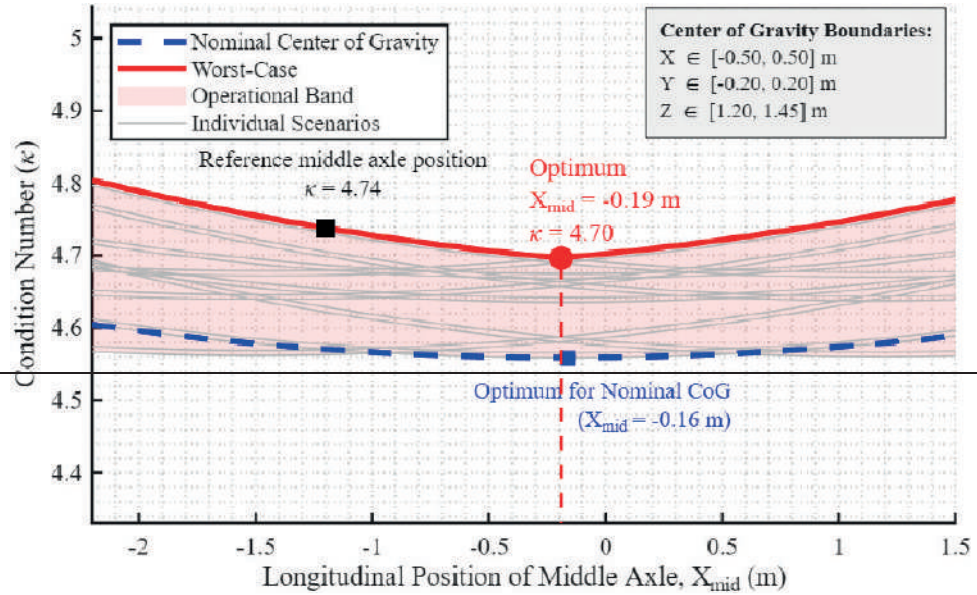
DOI: https://doi.org/10.30546/19023.978-9952-610-87-1.2026.100.1144.
ISBN: 978-9952-610-87-1

Figure 6a shows that when examining the system response under baseline uncertainty limits, the worst-case scenario condition number is $\kappa = 4.74$ at the reference position representing the rear axle placement (X_{mid}= -1.2 m). However, by shifting the center axle towards the geometric center of the chassis to the position X_{mid}= -0.19 m, this value is reduced to $\kappa = 4.70$, achieving the global optimum. Furthermore, it is noteworthy that the optimization based on the reference center of mass (blue square, X_{mid}= -0.16 m) and the robust center axle optimization encompassing all uncertainties (red circle, X_{mid}= -0.19 m) are quite close to each other. This convergence demonstrates that a design safe against worst-case scenarios does not compromise the vehicle's ideal performance.

In Figure 6 b, where the center of mass uncertainty limits is widened to push the optimization boundaries, the operational uncertainty band thickens, and the worst-case envelope is shifted upwards. These expanded centers of gravity position limits have increased the condition number of the reference or axle configuration to κ=4.95, and the condition number of the optimal point to κ=4.90. This mathematically confirms the imbalance created in the transmission matrix by extreme scenarios that asymmetrical stress the vehicle in the pitching and rolling directions, i.e., larger moment arms.

DOI: https://doi.org/10.30546/19023.978-9952-610-87-1.2026.100.1144.
ISBN: 978-9952-610-87-1

(a)



(b)

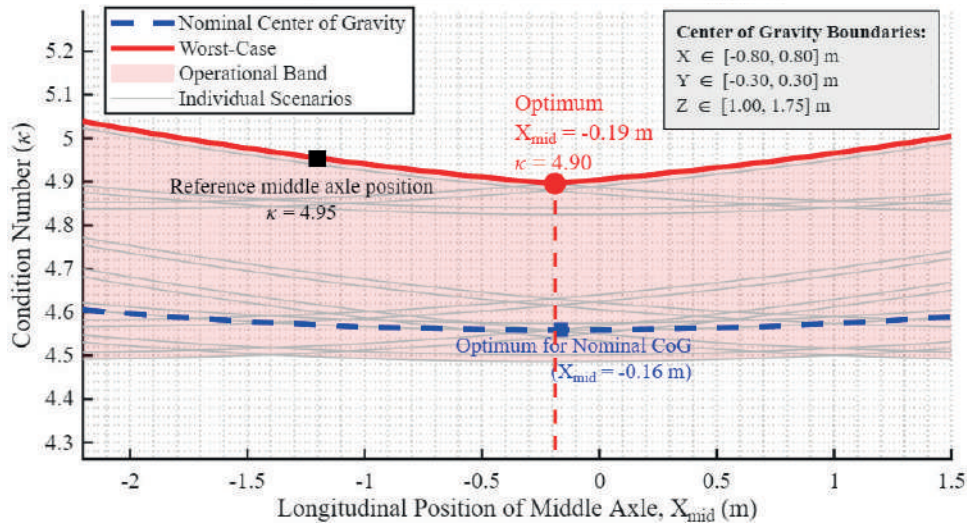


Figure 6. Middle axle optimization under two different center of gravity uncertainty boundaries: (a) narrow boundary, (b) extended boundary.

The most important finding of the comparative parametric results presented in Figure 6 is that, despite the expansion of operational uncertainty limits and the increase in system condition numbers, the optimum position remains unchanged at X_{mid}= -0.19 m. The fact that this obtained global optimum position differs from the just geometric center of the chassis (the geometric midpoint is X_{mid}= +0.10 m for front axle +2.8 m and rear axle -2.6 m) is a significant detail that reveals the success of the optimization model. The main reason for this deviation is that the algorithm focuses not only on axial distances but also on the dynamic moment effects created by the 3D mass distribution. The opposing tilting moments

Mx created by extreme scenarios where the mass reference point is located behind the chassis center and the center of gravity rises to 1.75 m on the Z-axis invalidate a simple geometric mean. Therefore, the algorithm does not consider the -0.19 m point as a mere distance average; It calculated the true kinematic and topological node as simultaneously damping the asymmetric distribution of weight and the opposing constraints imposed by the increase in height.

CONCLUSION

The decrease condition number associated with kinematic constraints in conventional commercial vehicles is often mitigated in Tactical Wheeled Armored Vehicles (TWVs) through advanced engineering solutions to meet high mobility requirements. The independent suspension architecture commonly used in modern TWVs reduces the dependence on traditional tandem linkages, offering designers greater flexibility to place the middle axle closer to the optimum (X_{mid} = -0.19 m) identified in the uncertainty analyses. Potential steering complexities, such as Ackermann geometry deviations caused by an increased wheelbase, can be compensated for by all-wheel steering systems.

The proposed SVD-based optimization model offers a quantitative perspective on the prevalent use of tandem configurations in commercial trucks and their associated trade-offs in topological stability. It mathematically highlights the geometric advantages of adopting more distributed, independent chassis architectures for modern armored platforms.

REFERENCES

Cheng, H., Hou, Z., Liu, Z., Li, J., Zhang, J., Zhao, Y., & Liu, X. (2026). Handling Stability Control for Multi-Axle Distributed Drive Vehicles Based on Model Predictive Control. *Vehicles, 8*(2), 26. Retrieved from https://www.mdpi.com/2624-8921/8/2/26

Duraikannu, D., & Dumpala, G. R. (2026). *High-Fidelity Modeling of Vehicle Dynamics for Control-Oriented Stability Enhancement.* Paper presented at the Symposium on International Automotive Technology (2026).

Fang, R., Shen, T., Bai, X., Liang, J., Wang, F., Zhuang, W., & Yin, G. (2025). Hierarchical Control With Steering Mode Switching for MDED-HDV via Maneuver Stability Region Analysis. *IEEE Transactions on Automation Science and Engineering, 22*, 23066–23082. doi:10.1109/TASE.2025.3613526

Hu, J., Li, J., Li, H., Dong, J., Hu, Z., Xu, L., & Ouyang, M. (2021). *Feedforward and feedback integrated control for handling characteristics adjustment of multi-axle heavy-duty vehicles using independent-drive electric wheels.* Paper presented at the 2021 5th CAA International Conference on Vehicular Control and Intelligence (CVCI).

Knupp, P. M. (2001). Algebraic mesh quality metrics. *SIAM journal on scientific computing, 23*(1), 193–218.

Liu, J., Chen, L., Li, H., Hu, Z., Li, J., & Ouyang, M. (2025, 24–26 Oct. 2025). *Simulation Analysis of the Roll-Yaw Coupled Safety Boundary for Multi-Axle Heavy-Duty Vehicles.* Paper presented at the 2025 9th CAA International Conference on Vehicular Control and Intelligence (CVCI).

Mantaras, D. A., Luque, P., & Alonso, M. (2022). Phase plane analysis applied to non-explicit multibody vehicle models. *Multibody System Dynamics, 56*(2), 173–188. doi:10.1007/s11044-022-09846-9

Meena, A., & Das, G. (2025). Advancements and Challenges in HydraulicSuspension Technologies for Half-Axle and Multi-Axle Vehicles: A Comprehensive Review.

Oliva, J., Goicolea, J. M., Antolín, P., & Astiz, M. Á. (2013). Relevance of a complete road surface description in vehicle–bridge interaction dynamics. *Engineering Structures, 56*, 466–476. doi:https://doi.org/10.1016/j.engstruct.2013.05.029

DOI: https://doi.org/10.30546/19023.978-9952-610-87-1.2026.100.1144.
ISBN: 978-9952-610-87-1

Wittmer, K., Sawodny, O., & Henning, K.-U. (2023). Model-Based Estimation of Vehicle Center of Gravity Height and Load. *Journal of Dynamic Systems, Measurement, and Control, 145*(5). doi:10.1115/1.4056987

Xu, X., Chen, G., Gao, X., Jiang, Y., & Feng, Y. (2023). Stability and energy-saving coordinated control strategy of six-wheel independent drive unmanned ground vehicle. *ISA Transactions, 143*, 692–706. doi:https://doi.org/10.1016/j.isatra.2023.10.001

Zhou, G., Kim, J., & Je Choi, Y. (2020). Jacobian approach to the kinestatic analysis of a full vehicle model with application to cornering motion analysis. *Proceedings of the Institution of Mechanical Engineers, Part C: Journal of Mechanical Engineering Science, 234*(18), 3543–3559.